Cancer associated fibroblast-dependent and -independent invasion of cancer cells

Ryotaro Kondo
The University of Tokyo
Naoya Sakamoto
National Cancer Center
Kenji Harada
National Cancer Center
Hiroko Hashimoto
National Cancer Center
Ryo Morisue
National Cancer Center
Kazuyoshi Yanagihara
National Cancer Center
Takahiro Kinoshita
National Cancer Center Hospital East
Motohiro Kojima
National Cancer Center
Genichiro Ishii (gishii@east.ncc.go.jp)
The University of Tokyo

Research Article

Keywords: cancer associated fibroblasts (CAFs), invasion, collagen, CAFs-dependent, CAFs-independent

Posted Date: October 14th, 2022

DOI: https://doi.org/10.21203/rs.3.rs-2148966/v1

Abstract

Purpose

Cancer cells are known to exhibit a cancer-associated fibroblast (CAF)-dependent invasive mode in the presence of CAFs. The purpose of this study was to investigate whether intrinsic factors of cancer cells influence the CAF-dependent invasive mode of cancer cells.

Methods

We observed the dynamic movement of CAFs and cancer cells by time-lapse imaging of 2-D and 3-D collagen invasion models and evaluated the invasion modes of gastric cancer cell lines (MKN-7, MKN-45, and HSC44PE). We further examined whether modification of the invasive capacity of CAFs can alter the invasive mode of MKN-7 and HSC44PE cells.

Results

When MKN-7 and MKN-45 were co-cultured with CAFs, CAFs first invade collagen matrix followed by cancer cells (CAF-dependent invasion), whereas HSC44PE invaded collagen matrix independently of CAFs invasion. Overexpression or suppression of podoplanin in CAFs, respectively increased or decreased the invasive capacity of CAFs themselves and significantly increased or decreased the number of invading MKN-7, respectively. CAFs overexpressing a podoplanin mutant lacking the cytoplasmic domain had a significantly reduced invasive capacity compared to CAFs overexpressing wild-type podoplanin, and it also reduced the number of invading MKN-7 cells significantly. When HSC44PE and CAFs were co-cultured, changes in the podoplanin expression in CAFs similarly altered the invasive capacity of CAFs themselves, but it did not affect the number of invading HSC44PE cells.

Conclusion

These results indicate that in the presence of CAFs, there are CAF-dependent and -independent modes of cancer cell invasion, the determinants of which may depend on the intrinsic properties of cancer cells.

Introduction

Tumor microenvironment is very complex composed of, not only cancer cells, but various types of stromal cells. Fibroblasts, a major component of tumor stromal cells are found to be associated with cancer cells, and hence known as cancer-associated fibroblasts (CAFs). CAFs have been reported to have a significant impact on cancer cell proliferation, local invasion, and metastasis through their interaction with cancer cells (Kalluri et al. 2006, Whatcott et al. 2013, Ishii et al. 2016).

The cancer stroma is filled with an extracellular matrix (ECM) composed mainly of type I collagen and the CAFs that produce it, which participate in the growth, migration and invasion of the cancer cells (Provenzano et al. 2008, Kakkad et al. 2010). Previous reports have revealed diverse morphologies and molecular mechanisms of cancer cell invasion into the stroma (Fridl et al. 2011). One of the modes of invasion into the stroma is single-cell invasion, in which invading single cancer cells exhibit a mesenchymal cell-like phenotype (Friedl et al. 2012). Other known modes of cancer cell invasion include collective invasion by numerous cancer cell groups that retain intercellular adhesions (Friedl et al. 2012, Novin et al. 2021).

On the other hand, in CAF-rich tumor microenvironments (TME), a CAF-dependent mode of cancer cell invasion is also known, in which CAFs first biomechanically remodel the collagen matrix, and subsequently cancer cells follow the CAFs and invade into the collagen matrix (Gaggioli et al. 2007, Neri et al. 2016, Miyashita et al. 2020). This CAF-dependent cancer cell invasion mode is associated with cell cycle progression in cancer cells and formation of small cancer cell nests (Miyashita et al. 2019). We previously reported that podoplanin-expressing CAFs have increased invasive potential as compared to normal CAFs due to their increased RhoA activity, which in turn increases the remodeled area of the ECM collagen and promotes local invasion of cancer cells (Neri et al. 2015). These previous findings indicate the possibility that in the CAF-rich TME, the ECM remodeling capacity of CAF has a significant impact on the invasive potential of cancer cells and that a cancer cell invasion mode dependent on CAF properties is the prevailing phenomenon (CAF-dependent cancer cell invasion).

In this study, we hypothesized that even in CAF-rich TMEs, the intrinsic factors of cancer cells may influence the CAF-dependent mode of cancer cell invasion. We investigated whether different gastric cancer cell lines have different invasion patterns using two-dimensional (2D) and three-dimensional (3D) invasion models that mimic the human TME, consisting of cancer cells, CAFs, and type I collagen (Nomura et al. 2022). We further examined whether endogenous modulation of the invasive potential of CAFs could alter the invasive mode of cancer cells within the 3D spheroids.

Materials And Methods

Cell culture

MKN-7 (gastric tubular adenocarcinoma) and MKN-45 (gastric adenocarcinoma) cells were obtained from the Japanese Collection of Research Bioresources Cell Bank and American Type Culture Collection, respectively. HSC44PE (gastric signet ring cell adenocarcinoma) (Yanagihara et al. 2004), MKN-7 and MKN-45 cells were cultured in RPMI 1640 (Sigma-Aldrich, St. Louis, MO, USA) medium supplemented with 10% fetal bovine serum (FBS; Life Technologies, New York, NY, USA) and 1% penicillin-streptomycin (P/S) solution (Sigma-Aldrich). Cells were incubated at 37°C in a humidified atmosphere containing 5% CO_2.

Fibroblast culture

Cancer associated fibroblasts (CAFs) were isolated from human gastric cancer tissue based on a previous report (Ishii T et al. 2021). CAFs were cultured in α-minimum essential medium (α-MEM; Life Technologies), supplemented with 10% FBS and 1% P/S solution, in a humidified atmosphere containing 5% CO_2 at 37°C. Fibroblast culture study was approved by the Institutional Review Board of the National Cancer Center (IRB number: 2005-043 and 2018 − 309).

Fluorescence labeling of gastric cancer cell lines

Lentiviruses were produced using 293T cells transfected with pCAG-HIV, pCMV-VSV-G-RSV-Rev, and CSII-CMV-mRFP1 vector (Riken BioResource Center, Japan), using Lipofectamine 2000 reagent (Invitrogen, NY, USA). Virus-containing medium was filtered through a 0.45 μm filter, and 8 μg/mL (final concentration) of polybrene (Santa Cruz, Dallas, TX, USA) was added for target cell transduction, as previously reported (Yamazaki et al. 2018). The mRFP-positive fractions of the gastric cancer cell lines were sorted by a FACS AriaII (BD Bioscience) (Fig. 1A) and were further cultured. We confirmed that over 90% of the cultured cells were mRFP-positive (Fig. 1B).

Lifetime extension of CAFs

Transduction was performed with human telomerase reverse transcriptase (*hTERT*) and mutant forms of cyclin-dependent kinase 4 (*CDK4R24C*) in combination (*hTERT/CDK4R24C*). *hTERT* and *CDK4R24C* cDNAs were kindly gifted by Dr. Masutomi K (Division of Cancer Stem Cells, National Cancer Center Research Institute) and Dr. Kiyono T (Division of Carcinogenesis and Cancer Prevention, National Cancer Center Research Institute), respectively. Using the packaging constructs PCAG-HIV, pCMV-VSV-G-RSV-Rev (RIKEN BioResource Center), CSII-CMV-hTERT-IRES2-Venus, and CSII-CMV-CDK4R24C-IRES2-Venus, infection was achieved as previously described (Hashimoto et al. 2017). The venus-positive fractions of CAFs were sorted and cultured further (Fig. 1C, left and middle). We confirmed increased levels of both *hTERT* and *CDK4* in CAFs (CAFs-hTERT/CDK4R24C) by qRT-PCR analysis (Fig. 1C, right). Primers used are listed in Supplementary Table 1.

*Two-dimensional (2D) collagen invasion assay (*Supplementary Fig. 1*)*

The 2D collagen invasion assay was performed as previously described (Miyashita et al. 2019). Briefly, CAFs and cancer cells was plated on a collagen (Cellmatrix Type -A; Nitta Gelatin)-coated (0.3% type I collagen gel) 96-well plates (Incucyte® Imagelock 96-well Plate: Sartorius, Germany) at a density of 1.15×10 cells/well (6.5×10⁴ cancer cells + 5.0×10⁴ CAFs). After 1 h incubation, we made a wound in the cell layer using 96-well WoundMaker (Sartorius), and embedded cells in type I collagen gel. Scratched field images were captured using the IncuCyte Live-Cell Imaging System (Sartorius).

Three-dimensional (3D) collagen invasion assay

To measure the invasiveness of cancer cells and CAFs in 3-dimensional (3D) culture mimicking the human TME, we first generated 3D hybrid cancer spheroids (Supplementary Fig. 2A) (Nomura et al. 2022). We prepared a cell mixture of 0.1 × 10⁴ gastric cancer cells (HSC44PE and MKN-7) and 0.9 × 10⁴ CAFs with extended lifespan. 1.0 × 10⁴ cells from this mixture was seeded onto 96-well low attachment

plates (Sumitomo Bakelite, Tokyo, Japan) and incubated overnight at 37°C. The medium was removed, and the cell aggregates were embedded in 50 µL collagen (Cellmatrix Type I-A; Nitta Gelatin, Oosaka, Japan) and incubated for 30 min at 37°C. After confirmation of polymerization of collagen, 100 µL of mixed medium (RPMI-1640: α-MEM = 1:1) was added. Time-lapse imaging analysis was performed using Incucyte (Sartorius) during incubation, and the medium was changed daily.

Evaluation of the number of cancer cells and CAFs invading the collagen gel discontinuously from the main spheroid

This evaluation was performed according to a previously described protocol (Nomura et al. 2022). We encircled the edge of the main spheroid on day 3 of culture on the bright-field image (orange solid line in Supplementary Fig. 2B, left), then, calculated the average distance between the center of gravity and edge of the cell cluster (the average of the center of gravity distance). We drew a circle with the center of gravity of the cell cluster as the center and a radius of four times the average of the center of gravity distance (orange dotted circle in Supplementary Fig. 2B, left). The circle on the bright-field image was reflected in the fluorescent image (orange dotted circle in Supplementary Fig. 2B, right). The number of cancer cells and CAFs invading the collagen gel discontinuously from the main spheroid in the circle were measured by WinROOF 2021 image analysis software (MITANI Corporation, Fukui, Japan).

Overexpression and knockdown of podoplanin of CAFs

To generate podoplanin or mutant podoplanin-overexpressing CAFs, lentiviruses were produced using 293T cells transfected with PCAG-HIV, pCMV-VSV-G-RSV-Rev, and either wild-type podoplanin (PDPN-WT) (kindly provided by Dr. N. Fujita, Japanese Foundation for Cancer Research), or mutant podoplanin lacking the cytoplasmic region (PDPN-Del.IC) (Supplementary Fig. 3A) (Martin-Villar et al. 2006, Ito et al. 2012).

To generate podoplanin-knockdown CAFs, two different short-hairpin RNA (shRNA) expression constructs, sh-podoplanin1 and sh-podoplanin 3, were created as previously described (Hoshino et al. 2011). An shRNA specific for the luciferase gene (sh-luciferase) was used as a control (Supplementary Fig. 3B).

Podoplanin expression analysis by flow cytometry

After incubation with an APC-conjugated anti-podoplanin antibody (clone NC-08, BioLegend, CA, USA), FACS analysis was performed using FACS Accuri C6 Plus (BD Biosciences)(Supplementary Fig. 3C and D).

Real-time reverse-transcriptase polymerase chain reaction (RT-PCR)

Total RNA was purified using the Nucleo Spin RNA Plus Kit (TaKaRa Bio, Osaka, Japan), and cDNA was synthesized using the PrimeScript RT Reagent Kit with gDNA Eraser (Takara Bio). RT-PCR was carried out on a Smart Cycler System (Takara Bio) with SYBR Premix Ex Taq (Takara Bio) and RT-PCR primers.

Information regarding the primers used is provided in Supplementary Table S1. Genes with CT values greater than 29 cycles (*vimentin* and *ZEB2*) were excluded from the analysis.

Statistical analysis

The significance of the differences between the two groups was evaluated using the Welch t-test. *P*-values were determined using two-sided analyses, and the statistical significance level was set at $P < 0.05$.

Results

Time lapse imaging analysis of two-dimensional (2D) collagen invasion assay

Using a 2D collagen invasion assay model, we investigated the invasion mode of the gastric cancer cell lines, MKN-7, MKN-45, and co-cultured CAFs. After 4 h, the CAFs began to infiltrate the collagen gel. Thereafter, the number and distance of invaded CAFs increased. MKN-7 and MKN-45 cells' invasion started 12 h later (Fig. 2A and B, arrowheads) following the CAFs. These results are consistent with those of previous studies (Gaggioli et al. 2007, Neri et al. 2016).

However, when HSC44PE cells were co-cultured with CAFs, both of them simultaneously infiltrated the collagen gel after 4 h (Fig. 2C, arrowheads) and both, the number and distance of infiltration increased with time. These results suggested that HSC44PE cells do not exhibit CAF-dependent invasion.

Time lapse imaging analysis of three-dimensional (3D) hybrid spheroid model

To study a model that better mimics the human TME, we used the 3D hybrid spheroid model that we developed earlier (Nomura et al. 2022). When MKN-7 and MKN-45 cells were co-cultured with CAFs, CAFs invasion was first observed after 24 h (Fig. 3A and B, arrows). MKN-7 and MKN-45 cells began to infiltrate after 32 and 40 h later, respectively (Fig. 3A and B, arrowheads). When HSC44PE cells and CAFs were co-cultured, HSC44PE cells first showed invasion after 16 h (Fig. 3C, arrow heads), and CAFs started invading after 24 h (Fig. 3C, arrows). The number of invading HSC44PE cells after 48 h was much higher than that of MKN-7 and MKN-45 cells.

Invasive ability of CAFs overexpressing podoplanin and MKN-7 cells in 3D hybrid spheroid model

We have previously reported that podoplanin overexpression in CAFs increases the invasive potential of CAFs via enhanced RhoA activation, which in turn increases the number of invasive cancer cells (Neri et al. 2015). CAFs overexpressing wild-type podoplanin (CAFs-PDPN-WT), and MKN-7 were co-cultured, and the number of CAFs, and MKN-7 cells infiltrating into the collagen gel were measured after 72 h (Fig. 4A, left). The average number of invaded CAFs and MKN-7 cells was 1.4- and 1.3-fold higher, respectively,

than the control CAFs (CAFs-Ctrl) ($p < 0.01$) (Fig. 4B and 4C). CAFs overexpressing the podoplanin mutant with deleted cytoplasmic domain (CAFs-PDPN-Del.IC) had a significantly reduced invasive capacity (0.73-fold) compared to CAFs overexpressing wild-type podoplanin (Fig. 4A and B). The number of infiltrated MKN-7 cells was also significantly reduced (0.78-fold) (Fig. 4A and C).

Invasive ability of CAFs overexpressing podoplanin and HSC44PE cells in 3D hybrid spheroid model

Next, we performed the same experiment using HSC44PE cells. Overexpression of podoplanin in CAFs increased the invasive capacity of CAFs by 2.0-fold and podoplanin-Del.IC decreased the invasive capacity of CAFs by 0.7-fold (both $p < 0.01$) (Fig. 4A, right, and D). In contrast, unlike MKN-7 cells, the number of invading HSC44PE cells did not depend on the amount of podoplanin expression in CAFs (Fig. 4A right and E).

Invasive ability of CAFs with suppressed podoplanin expression and MKN-7 cells in a 3D hybrid spheroid model

Using 3D-spheroid composed exclusively of CAFs, we compared the invasive capacity of CAFs with suppressed podoplanin expression (CAFs-Luc vs. CAFs-shPDPN1 and -sh3). Knockdown of podoplanin significantly reduced the number of CAFs infiltrated by 0.7- and 0.8-fold for shPDPN1 and shPDPN3, respectively (shLuc vs. shPDPN1, $p < 0.01$, shLuc vs. shPDPN3, $p < 0.05$) (Supplementary Fig. 4A and B). MKN-7 cells were then co-cultured with CAFs-shPDPN1 and shPDPN3, and the invasive numbers of CAFs and MKN-7 cells were examined. As shown in Fig. 5, podoplanin knockdown significantly inhibited the invasive number of both CAFs and MKN-7 cells (Fig. 5A, left, B, and C).

Invasive ability of CAFs with suppressed expression of podoplanin and HSC44PE cells in a 3D hybrid spheroid model

The same experiment when conducted using HSC44PE cells showed that knockdown of podoplanin significantly suppressed the invasive potential of CAFs (Fig. 5A right and D) but did not affect the invasive potential of HSC44PE (Fig. 5A right and E).

Discussion

It is well known that in TMEs where CAFs are abundant, CAF-dependent local invasion is a predominant process by which cancer cell invade the ECM using physically remodeled tracks by CAFs (Gaggioli et al. 2007, Neri et al. 2016, Miyashita et al. 2020). Previous studies have shown that changes in the properties of CAFs, such as altering their invasive potential can affect their invasive potential in cancer cells. For example, Neri et al. showed using 2D model, that CAFs with podoplanin overexpression enhance the invasive potential of CAFs themselves, resulting in ECM remodeling and enhanced A549 cell (lung adenocarcinoma cell line) invasion (Neri et al. 2015). In the current study, by observing dynamic movement of cancer cells and CAFs within the 2D and 3D models, we concluded that MKN-7 cells exhibit

a CAF-dependent invasion mode, while HSC44PE cells exhibit a CAF-independent invasion mode. This was further confirmed by the observation that, the ability of CAFs to remodel by overexpressing or suppressing podoplanin correlated positively with the number of infiltrating MKN-7 cells but not with the number of infiltrating HSC44PE cells.

Human podoplanin is a 38 kDa type-1 transmembrane glycoprotein and consists of 162 amino acids, nine of which form an intracellular domain (Krishnan et al. 2018). The podoplanin intracellular domain regulates RhoA activity *via* the ERM binding motif (Martin et al. 2006) and facilitates the invasion ability of CAFs (Neri et al. 2015). CAFs expressing mutant podoplanin lacking the cytoplasmic region (PDPN-Del.IC) invaded the collagen matrix less than CAFs overexpressing PDPN-WT (Neri et al. 2015). Correspondingly, the number of invaded MKN-7 cells co-cultured with CAFs overexpressing PDPN-Del.IC was significantly suppressed. These results suggest that CAF-dependent invasive mode of MKN-7 cells is unlikely to be due to the interaction of podoplanin expressed on the CAFs and podoplanin ligand expressed on cancer cells, rather supporting previous reports that the remodeled region of the ECM by CAFs determines the invasive potential of cancer cells.

Why did HSC44PE cells not exhibit a CAF-dependent invasion mode? The following may be the possible reasons. First, the interaction with CAFs via extrinsic factors, such as soluble factors, induce a CAF-independent invasion pattern in HSC44PE cells. A second possibility is that intrinsic factors in cancer cells themselves are determinants of the CAF-dependent or CAF-independent mode of cancer cell invasion. HSC44PE is a cancer cell line established from the body fluids of patients with gastric scirrhous carcinoma and has been reported to form highly invasive tumors (Yanagihara et al. 2004, Yanagihara et al. 2005). It is possible that only the intrinsic properties of the cancer cells, such as protease activity and Rho activating function, may be responsible for the cancer cell invasion mode and not the properties of CAFs.

A previous study reported that epithelial-mesenchymal transition (EMT) of cancer cells affects CAF-dependent local invasion (Neri et al. 2017). Platelet-derived growth factor (PDGF)-B secretion was elevated in cancer cells undergoing EMT, which induced an increase in the invasion ability of both cancer cells and CAFs. In this study, the expression of EMT-related mRNAs except Snail in HSC44PE cells was not higher than that in MKN-7 and MKN-45 cells. Moreover, the expression level of PDGF-B in HSC44PE cells was lower than that in MKN-7 cells (Supplementary Fig. 5). Based on these results, the EMT of cancer cells does not seem to be a decisive factor for CAF-independent invasion.

In conclusion, both CAF-dependent and CAF-independent modes of cancer cell invasion exist within a TME enriched with CAFs, the determinants of which may depend on the intrinsic nature of the cancer cells (Fig. 6). This supports the possibility that, even within the same tumor, there is a mixture of cancer cell subtypes that exhibit CAF-dependent and CAF-independent modes of invasion. Furthermore, the present results provide important clues for understanding the heterogeneity of cancer cell invasive potential within a fibrous TME.

Declarations

Acknowledgment

We would like to thank Editage (www.editage.com) for English language editing

There are no conflicts of interest to declare.

Author contributions

Ryotaro Kondo: Writing – original draft, Methodology, Formal analysis, Investigation, Data curation.

Naoya Sakamoto: Methodology, Formal analysis, Data curation, Writing – Review & Editing.

Kenji Harada: Methodology, Investigation, Data curation, Writing – Review & Editing

Hiroko Hashimoto: Methodology, Investigation, Writing – Review & Editing.

Ryo Morisue: Data curation, Writing – Review & Editing.

Kazuyoshi Yanagihara: Methodology, Writing – Review & Editing.

Takahiro Kinoshita: Methodology, Writing – Review & Editing.

Motohiro Kojima: Data curation, Writing – Review & Editing.

Genichiro Ishii: Conceptualization, Methodology, Data curation, Writing – original draft, Supervision, Project administration, and Funding acquisition.

Funding: This study was supported in part by the National Cancer Center Research and Development Fund [2020-A-9] and JSPS KAKENHI [21H02931].

References

1. Asif PJ, Longobardi C, Hahne M, Medema JP (2021) The Role of Cancer-Associated Fibroblasts in Cancer Invasion and Metastasis. Cancers (Basel) 13(18):4720 https://doi: 10.3390/cancers13184720.
2. Czekay RP, Cheon DJ, Samarakoon R, Kutz SM, Higgins PJ (2022) Cancer-Associated Fibroblasts: Mechanisms of Tumor Progression and Novel Therapeutic Targets. Cancers (Basel) 14(5):1231 https://doi: 10.3390/cancers14051231.
3. Friedl P, Alexander S (2011) Cancer invasion and the microenvironment: plasticity and reciprocity. Cell 147(5):992-1009 https://doi: 10.1016/j.cell.2011.11.016.
4. Friedl P, Locker J, Sahai E, Segall JE (2012) Classifying collective cancer cell invasion. Nat Cell Biol 14(8):777-83 https://doi: 10.1038/ncb2548.

5. Gaggioli C, Hooper S, Hidalgo-Carcedo C, Grosse R, Marshall JF, Harrington K, Sahai E (2007) Fibroblast-led collective invasion of carcinoma cells with differing roles for RhoGTPases in leading and following cells. Nat Cell Biol (12):1392-400 https://doi: 10.1038/ncb1658.
6. Hashimoto H, Suda Y, Miyashita T, Ochiai A, Tsuboi M, Masutomi K, Kiyono T, Ishii G (2017) A novel method to generate single-cell-derived cancer-associated fibroblast clones. J Cancer Res Clin Oncol 143(8):1409-1419 https://doi: 10.1007/s00432-017-2409-3.
7. Hoshino A, Ishii G, Ito T, Aoyagi K, Ohtaki Y, Nagai K, Sasaki H, Ochiai A (2011) Podoplanin-positive fibroblasts enhance lung adenocarcinoma tumor formation: podoplanin in fibroblast functions for tumor progression. Cancer Res 71(14):4769-4779 https://doi.org/10.1158/0008-5472.CAN-10-3228.
8. Ishii G, Ochiai A, Neri S (2016) Phenotypic and functional heterogeneity of cancer-associated fibroblast within the tumor microenvironment. Adv Drug Deliv Rev 99(Pt B):186-96 https://doi: 10.1016/j.addr.2015.07.007.
9. Ishii T, Suzuki A, Kuwata T, Hisamitsu S, Hashimoto H, Ohara Y, Yanagihara K, Mitsunaga S, Yoshino T, Kinoshita T, Ochiai A, Shitara K, Ishii G (2021) Drug-exposed cancer-associated fibroblasts facilitate gastric cancer cell progression following chemotherapy. Gastric Cancer 24(4):810-822 https://doi: 10.1007/s10120-021-01174-9.
10. Ito S, Ishii G, Hoshino A, Hashimoto H, Neri S, Kuwata T, Higashi M, Nagai K, Ochiai A (2012) Tumor promoting effect of podoplanin-positive fibroblasts is mediated by enhanced RhoA activity. Biochem Biophys Res Commun 422(1):194-9 https://doi: 10.1016/j.bbrc.2012.04.158.
11. Kakkad SM, Solaiyappan M, O'Rourke B, Stasinopoulos I, Ackerstaff E, Raman V, Bhujwalla ZM, Glunde K (2010) Hypoxic tumor microenvironments reduce collagen I fiber density. Neoplasia 12(8):608-17 https://doi: 10.1593/neo.10344.
12. Kalluri R, Zeisberg M (2006) Fibroblasts in cancer. Nat Rev Cancer 6:392-401 https://doi: org/10.1038/nrc1877.
13. Krishnan H, Rayes J, Miyashita T, Ishii G, Retzbach EP, Sheehan SA, Takemoto A, Chang YW, Yoneda K, Asai J, Jensen L, Chalise L, Natsume A, Goldberg GS (2018) Podoplanin: An emerging cancer biomarker and therapeutic target. Cancer Sci 109(5):1292-1299 https://doi: 10.1111/cas.13580.
14. Labernadie A, Kato T, Brugués A, Serra-Picamal X, Derzsi S, Arwert E, Weston A, González-Tarragó V, Elosegui-Artola A, Albertazzi L, Alcaraz J, Roca-Cusachs P, Sahai E, Trepat X (2017) A mechanically active heterotypic E-cadherin/N-cadherin adhesion enables fibroblasts to drive cancer cell invasion. Nat Cell Biol 19(3):224-237 https://doi: 10.1038/ncb3478.
15. Martín-Villar E, Megías D, Castel S, Yurrita MM, Vilaró S, Quintanilla M (2006) Podoplanin binds ERM proteins to activate RhoA and promote epithelial-mesenchymal transition. J Cell Sci 119(Pt 21):4541-53 https://doi: 10.1242/jcs.03218.
16. Miyashita T, Neri S, Hashimoto H, Akutsu A, Sugano M, Fujii S, Ochiai A, Ishii G (2020) Fibroblasts-dependent invasion of podoplanin-positive cancer stem cells in squamous cell carcinoma. J Cell Physiol 235(10):7251-7260 https://doi: 10.1002/jcp.29624.

17. Miyashita T, Omori T, Nakamura H, Sugano M, Neri S, Fujii S, Hashimoto H, Tsuboi M, Ochiai A, Ishii G (2019) Spatiotemporal characteristics of fibroblasts-dependent cancer cell invasion. J Cancer Res Clin Oncol 145(2):373-381 https://doi: 10.1007/s00432-018-2798-y.
18. Mohammadi H, Sahai E (2018) Mechanisms and impact of altered tumour mechanics. Nat Cell Biol 20(7):766-774 https://doi: 10.1038/s41556-018-0131-2.
19. Neri S, Hashimoto H, Kii H, Watanabe H, Masutomi K, Kuwata T, Date H, Tsuboi M, Goto K, Ochiai A, Ishii G (2016) Cancer cell invasion driven by extracellular matrix remodeling is dependent on the properties of cancer-associated fibroblasts. J Cancer Res Clin Oncol 142(2):437-46 https://doi: 10.1007/s00432-015-2046-7.
20. Neri S, Ishii G, Hashimoto H, Kuwata T, Nagai K, Date H, Ochiai A (2015) Podoplanin-expressing cancer-associated fibroblasts lead and enhance the local invasion of cancer cells in lung adenocarcinoma. Int J Cancer 137(4):784-96 https://doi: 10.1002/ijc.29464.
21. Neri S, Miyashita T, Hashimoto H, Suda Y, Ishibashi M, Kii H, Watanabe H, Kuwata T, Tsuboi M, Goto K, Menju T, Sonobe M, Date H, Ochiai A, Ishii G (2017) Fibroblast-led cancer cell invasion is activated by epithelial-mesenchymal transition through platelet-derived growth factor BB secretion of lung adenocarcinoma. Cancer Lett 395:20-30 https://doi: 10.1016/j.canlet.2017.02.026.
22. Nomura K, Nakai T, Nishina Y, Sakamoto N, Miyoshi T, Tane K, Samejima J, Aokage K, Kojima M, Sakashita S, Taki T, Miyazaki S, Watanabe R, Suzuki K, Tsuboi M, Ishii G (2022) 18F-fluorodeoxyglucose uptake in PET is associated with the tumor microenvironment in metastatic lymph nodes and prognosis in N2 lung adenocarcinoma. Cancer Sci 113(4):1488-1496 https://doi: 10.1111/cas.15266.
23. Novin A, Suhail Y, Ajeti V, Goyal R, Wali K, Seck A, Jackson A, Kshitiz (2021) Diversity in cancer invasion phenotypes indicates specific stroma regulated programs. Hum Cell 34(1):111-121 https://doi: 10.1007/s13577-020-00427-6.
24. Provenzano PP, Inman DR, Eliceiri KW, Knittel JG, Yan L, Rueden CT, White JG, Keely PJ (2008) Collagen density promotes mammary tumor initiation and progression. BMC Med 28;6:11 https://doi: 10.1186/1741-7015-6-11.
25. Sharma V, Letson J, Furuta S (2022) Fibrous stroma: Driver and passenger in cancer development. Sci Signal 15(724):eabg3449 https://doi: 10.1126/scisignal.abg3449.
26. Suzuki J, Tsuboi M, Ishii G (2022) Cancer-associated fibroblasts and the tumor microenvironment in non-small cell lung cancer. Expert Rev Anticancer Ther 22(2):169-182 https://doi: 10.1080/14737140.2022.2019018.
27. Whatcott C, Han H, Posner RG, Von Hoff DD (2013) Tumor-stromal interactions in pancreatic cancer. Crit Rev Oncog 18(1-2):135-51 https://doi: 10.1615/critrevoncog.v18.i1-2.80.
28. Yamazaki S, Higuchi Y, Ishibashi M, Hashimoto H, Yasunaga M, Matsumura Y, Tsuchihara K, Tsuboi M, Goto K, Ochiai A, Ishii G (2018) Collagen type I induces EGFR-TKI resistance in EGFR-mutated cancer cells by mTOR activation through Akt-independent pathway. Cancer Sci 109(6):2063-2073 https://doi: 10.1111/cas.13624.

29. Yanagihara K, Takigahira M, Tanaka H, Komatsu T, Fukumoto H, Koizumi F, Nishio K, Ochiya T, Ino Y, Hirohashi S (2005) Development and biological analysis of peritoneal metastasis mouse models for human scirrhous stomach cancer. Cancer Sci 96(6):323-32 https://doi: 10.1111/j.1349-7006.2005.00054.x.
30. Yanagihara K, Tanaka H, Takigahira M, Ino Y, Yamaguchi Y, Toge T, Sugano K, Hirohashi S (2004) Establishment of two cell lines from human gastric scirrhous carcinoma that possess the potential to metastasize spontaneously in nude mice. Cancer Sci 95(7):575-82 https://doi: 10.1111/j.1349-7006.2004.tb02489.x.

Figures

Figure 1

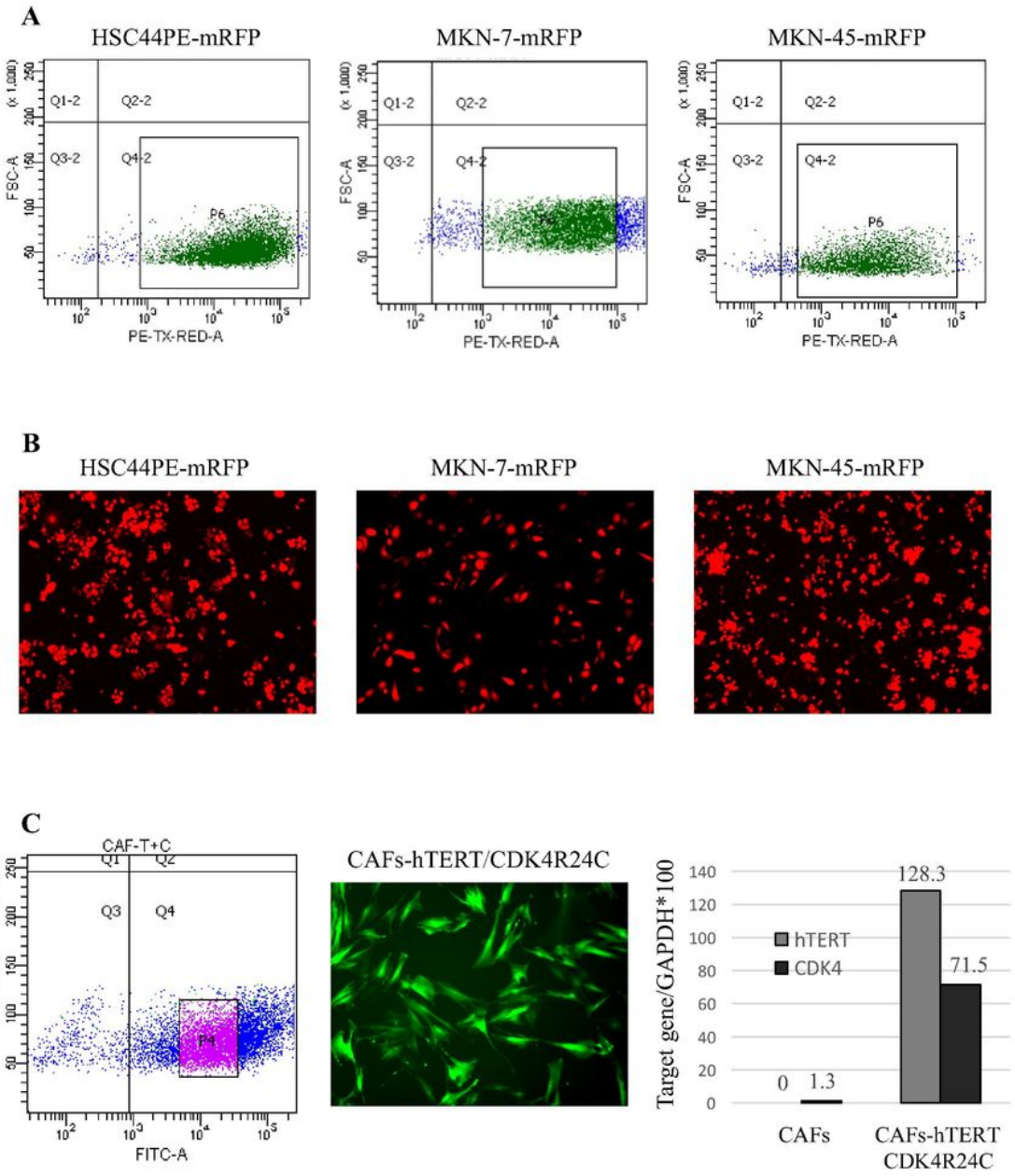

Figure 1

Cells used in this study

A: mRFP labelling of three gastric cancer cell lines. The areas enclosed by squares were sorted.

B: mRFP-positive cultured cells grown after sorting

C: Lifetime extension of gastric cancer tissue-derived CAFs. The area enclosed by the square is sorted after lentiviral transfection (left). Venus-positive CAFs after sorting (middle). RT-PCR analysis of exogenous hTERT/CDK4R24C transduction (right).

Figure 2

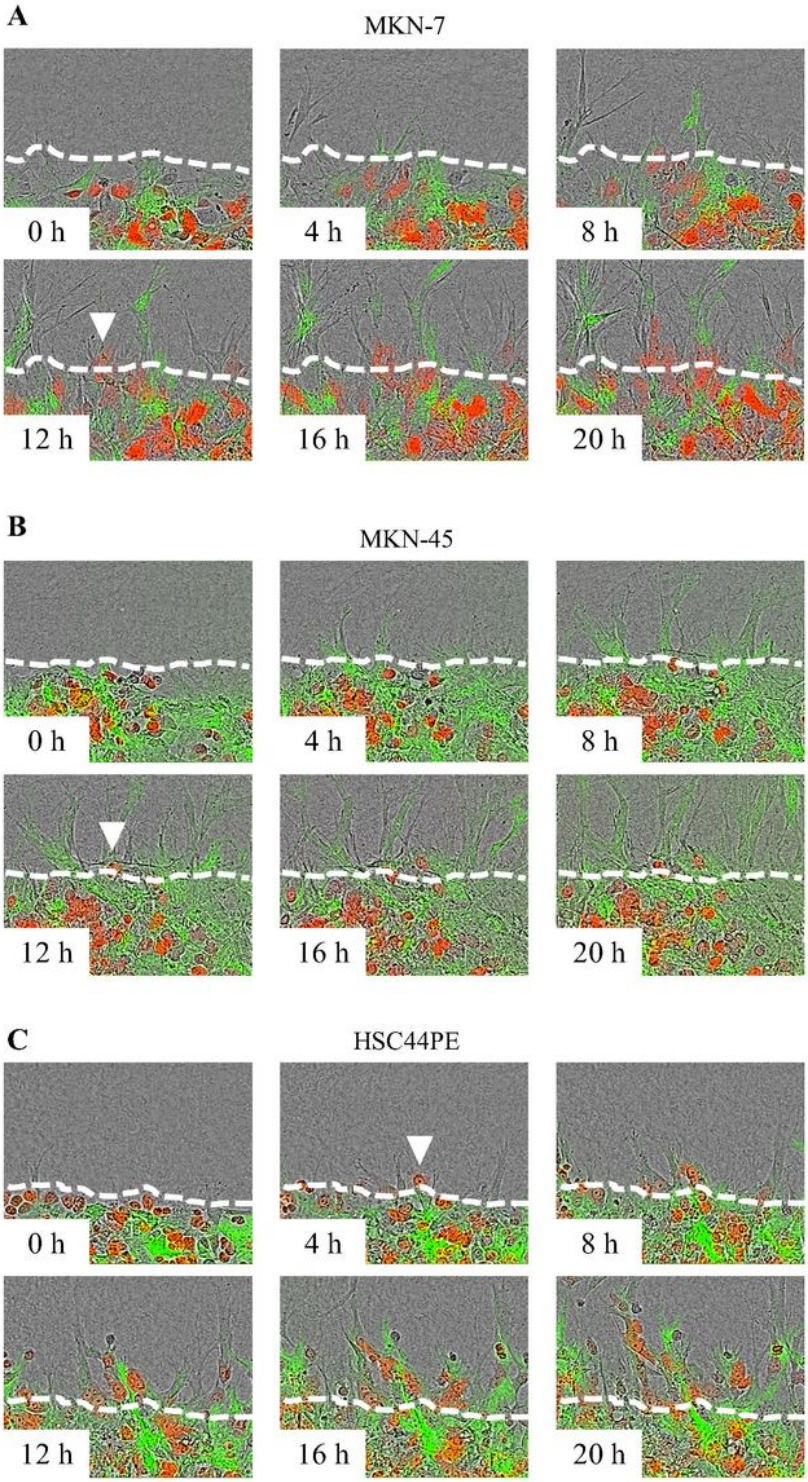

Figure 2

Two-dimensional (2D) collagen invasion assay

A: Representative time-lapse images of co-cultures of MKN-7 cancer cells(red) and CAFs (green). Arrowheads indicate the cancer cells that have begun to invade.

B: Representative time-lapse images of co-cultures of MKN-45 cancer cells(red) and CAFs (green). Arrowheads indicate the cancer cells that have begun to invade.

C: Representative time-lapse images of co-cultures of HSC44PE cancer cells (red) and CAFs (green). Arrowheads indicate the cancer cells that have begun to invade.

Figure 3

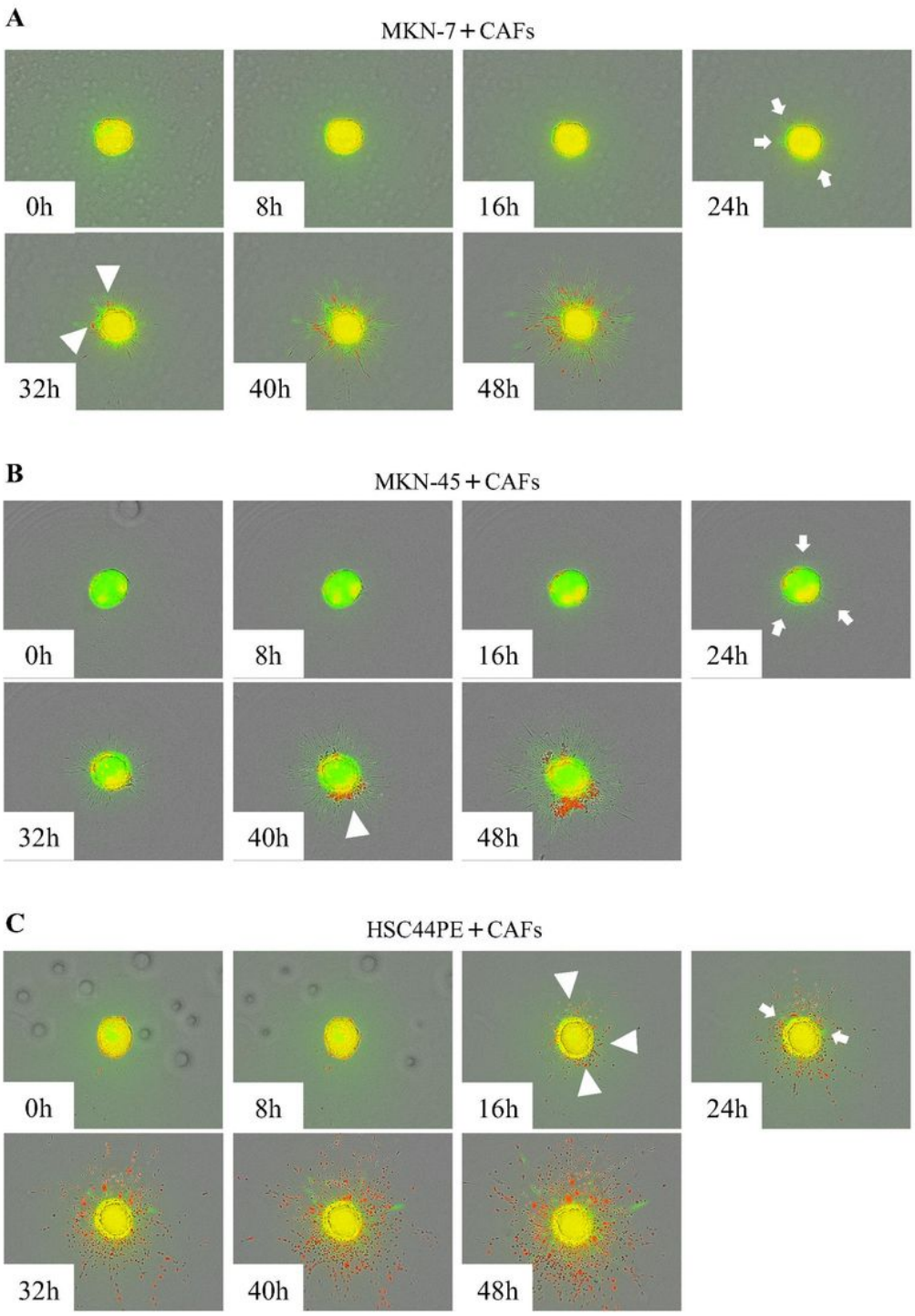

Figure 3

Three-dimensional (3D) collagen invasion assay

A: Representative time-lapse images of co-cultures of MKN-7 cancer cells(red) and CAFs (green). Arrows and arrowheads indicate CAFs and MKN-7 cancer cells that have initiated invasion, respectively.

B: Representative time-lapse images of co-cultures of MKN-45 cancer cells(red) and CAFs (green). The arrows and arrowheads indicate CAFs and MKN-45 cancer cells that have initiated invasion, respectively.

C: Representative time-lapse images of co-cultures of HSC44PE cancer cells (red) and CAFs (green). The arrows and arrowheads indicate CAFs and HSC44PE cancer cells that have initiated invasion, respectively.

Figure 4

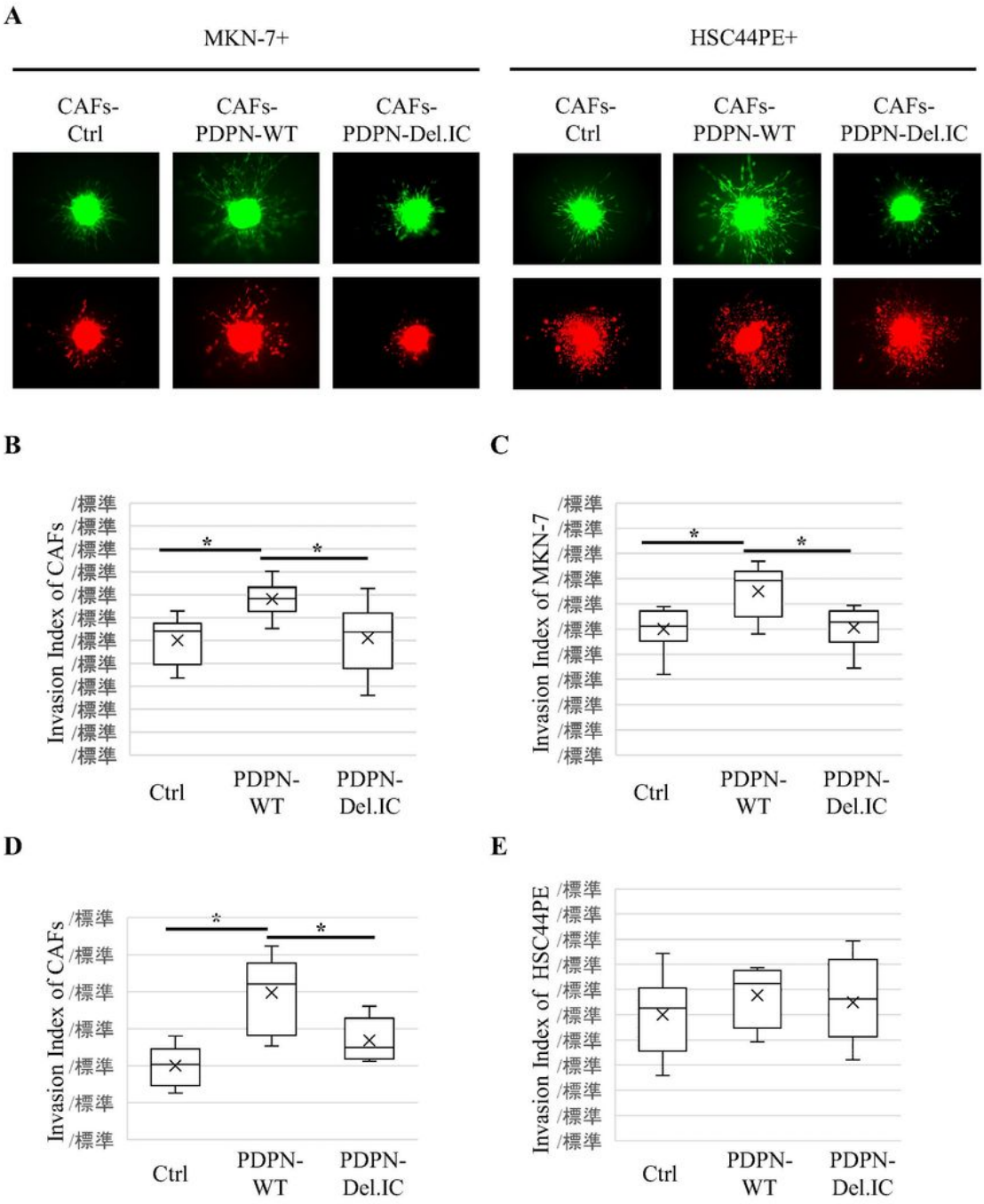

Figure 4

CAFs overexpressing podoplanin (PDPN) promote invasion of MKN-7 cancer cells but not HSC44PE cancer cells in 3D collagen invasion assay

A: Representative images (72 h) of the co-cultures of cancer cells and CAFs-Ctrl; CAFs overexpressing PDPN (CAFs-PDPN-WT), and CAFs overexpressing mutant PDPN (CAFs-PDPN -Del.IC). Green and red cells represent CAFs and cancer cells, respectively.

B: Comparison of the invasion number of CAFs-ctrl (n=11); CAFs-PDPN-WT (n=10); and CAFs-PDPN -Del.IC (n=10) when co-cultured with MKN-7 cells. The invasion index of CAFs on the y-axis indicates the number of invasions when Ctrl is set to 1. *p<0.01

C: Comparison of the number of invading MKN-7 cancer cells when co-cultured with CAFs-ctrl (n=10), CAFs-PDPN-WT (n=11), and CAFs-PDPN-Del.IC (n=10). The invasion index of MKN-7 on the y-axis indicates the number of invasions when Ctrl is set to 1. *p<0.01

D: Comparison of the number of invading CAFs-ctrl (n=10), CAFs-PDPN-WT (n=7), and CAFs-PDPN-Del.IC (n=8) when co-cultured with HSC44PE cells. The invasion index of CAFs on the y-axis indicates the number of invasions when Ctrl is set to 1. *p<0.01

E: Comparison of the number of invading HSC44PE cancer cells when co-cultured with CAFs-ctrl (n=10), CAFs-PDPN-WT (n=6), and CAFs-PDPN-Del.IC (n=7). The invasion index of HSC44PE on the y-axis indicates the number of invasions when Ctrl is set to 1. *p<0.01

Figure 5

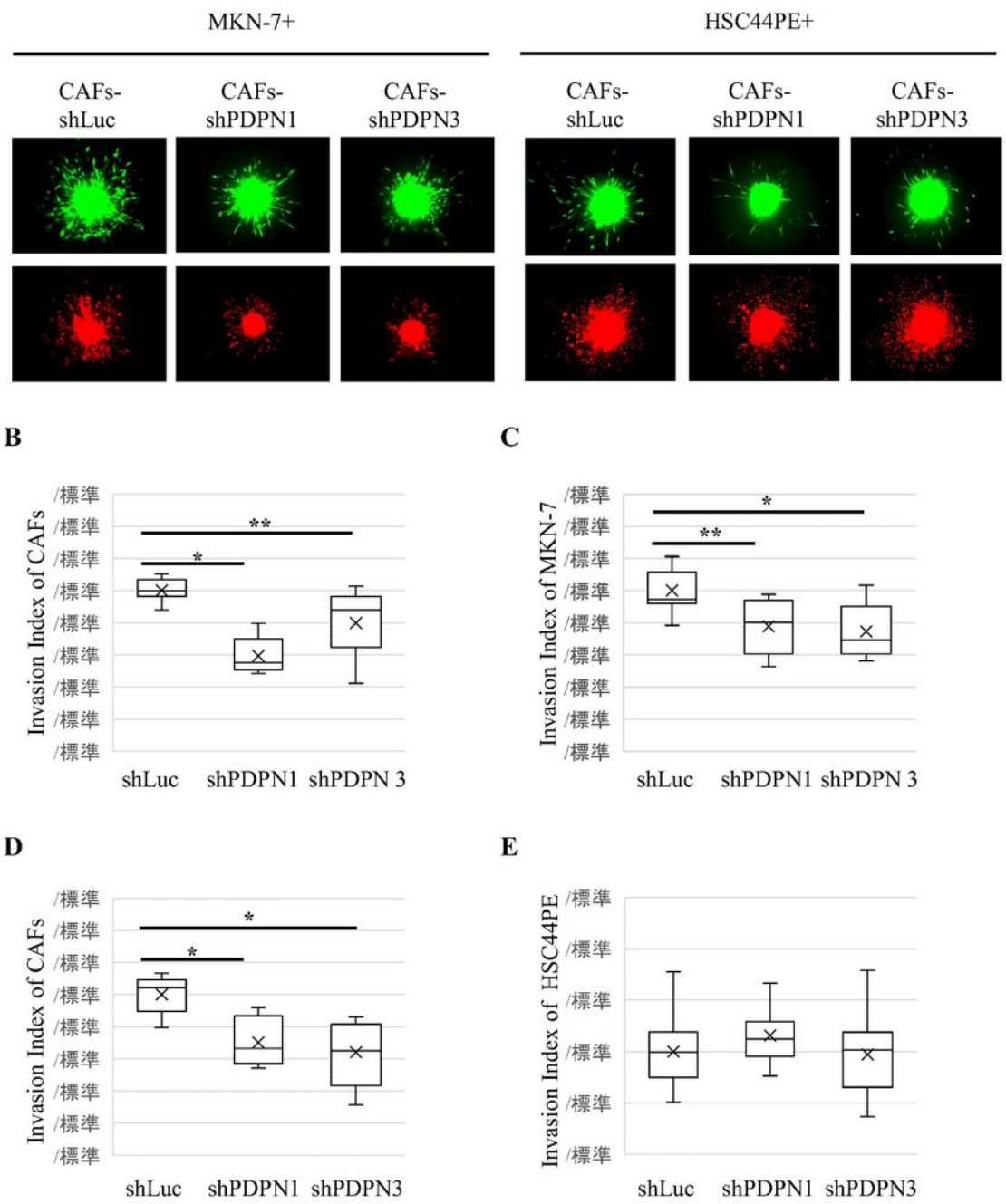

Figure 5

CAFs with suppressed PDPN expression inhibit invasion of MKN-7 cancer cells but not HSC44PE cancer cells in 3D collagen invasion assay

A: Representative images (72 h) of the co-cultures of cancer cells and CAFs-shLuc and CAFs with suppressed PDPN expression (CAFs-shPDPN1 and CAFs-shPDPN3). Green and red cells represent CAFs

and cancer cells, respectively.

B: Comparison of the invasion number of CAFs-shLuc (n=7), CAFs-shPDPN1 (n=6), and CAFs-shPDPN3 (n=7) cells when co-cultured with MKN-7 cancer cells. The invasion index of CAFs on the y-axis indicates the number of invasions when shLuc is set to 1. *p<0.01, **p<0.05

C: Comparison of the invasion number of MKN-7 cancer cells when co-cultured with CAFs-Luc (n=7), CAFs-shPDPN1 (n=6), and CAFs-shPDPN3 (n=8). The invasion index of MKN-7 on the y-axis indicates the number of invasions when shLuc is set to 1. *p<0.01, **p<0.05

D: Comparison of the invasion number of CAFs-shLuc (n=10), CAFs-shPDPN1 (n=8), and CAFs-shPDPN3 (n=11) cells when co-cultured with HSC44PE cancer cells. The invasion index of CAFs on the y-axis indicates the number of invasions when shLuc is set to 1. *p<0.01

E: Comparison of the invasion number of HSC44PE cancer cells when co-cultured with CAFs-shLuc (n=11), CAFs-shPDPN1 (n=10), and CAFs-shPDPN3 (n=14). The invasion index of HSC44PE on the y-axis indicates the number of invasions when shLuc is set to 1.

Figure 6

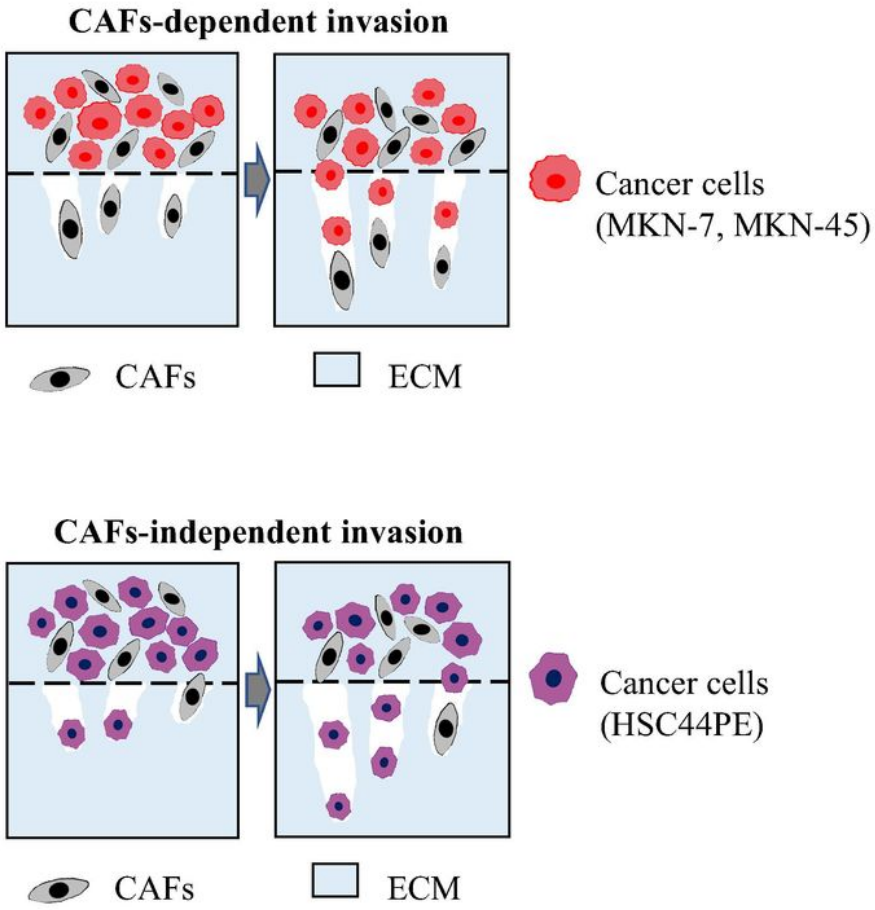

Figure 6

Scheme of CAF-dependent and CAF-independent modes of cancer cell invasion.

Upper figure: When MKN-7 and MKN-45 cells were seeded with CAFs, CAFs first invaded the ECM, followed by MKN-7 and MKN-45 cells (CAFs- dependent invasion).

Lower figure: When HSC44PE cells were seeded with CAFs, HSC44PE cells invaded the ECM independently of CAFs invasion (CAF-independent invasion).

ECM; extracellular matrix

Supplementary Files

This is a list of supplementary files associated with this preprint. Click to download.

- SuppFigure.pptx
- Table.pptx